THE ASTROPHYSICAL JOURNAL, 271:672–680, 1983 August 15


# CHROMOSPHERIC AND CORONAL EMISSIONS FROM THE GIANTS IN THE HYADES

S. L. BALIUNAS,[1] L. HARTMANN,[1] AND A. K. DUPREE[1]
Harvard-Smithsonian Center for Astrophysics
*Received 1982 September 13; accepted 1983 January 27*

## ABSTRACT

We have measured the visible Ca II K and *International Ultraviolet Explorer* spectra from the four K0 III stars ($\theta^1$, $\gamma$, $\delta$, and $\varepsilon$ Tau) in the Hyades, along with a field giant of similar spectral type, $\beta$ Gem. Among the Hyades giants, the range of the high-temperature emissions can be a factor of 6 or more for C IV and an order of magnitude in the X-ray luminosity measured by Stern *et al.* For these presumably coeval cluster giants with similar macroscopic parameters, such as age, mass, effective temperature, gravity, and projected rotational velocity, the observed range in chromospheric and coronal emissions is not easily explained by the dominant factors thought to control these emissions in cool stars. It is possible that the emissions are time variable, on a time scale longer than six months. This would be the first evidence that giants undergo magnetic activity cycles similar to those of dwarf stars.

*Subject headings:* Ca II emission — clusters: open — stars: chromospheres — stars: late-type — stars: coronae — ultraviolet: spectra

## I. INTRODUCTION

The study of stars in the galactic cluster nearest the Sun, the Hyades, presents a unique opportunity to explore chromospheric and coronal emissions in late-type stars. For the cluster stars, which are believed to be coeval, certain parameters thought to affect the chromospheric emissions can be explored. Among the optically brightest members of the cluster are four evolved stars near spectral type K0 III. These giants, while not identical, are relatively similar in effective temperatures, gravities, masses, and metallicities (Boesgaard, Heacox, and Conti 1977; Keenan and Pitts 1980; Lambert, Dominy and Sivertsen 1980; Gray and Endal 1982). With this homogeneous sample of stars, we can examine an average level of chromospheric and coronal emission as a function of macroscopic parameters. We compare chromospheric spectra of Ca II K, Mg II $h$ and $k$, and ultraviolet transition-region spectra along with reported X-ray luminosities of the Hyades giants.

## II. OBSERVATIONS

We observed Mg II $h$ and $k$ and Ca II K profiles and solar-like transition-region emissions from the four Hyades giants, $\theta^1$ (77) Tau, $\gamma$ Tau, $\delta$ Tau, and $\varepsilon$ Tau, and the field star $\beta$ Gem. The ultraviolet observations from *International Ultraviolet Explorer* (*IUE*) consist of high-resolution ($\sim 0.2$ Å) profiles of the Mg II $h$ and $k$ ($\lambda 2800$) features and the short-wavelength, low-resolution ($\sim 6$ Å) spectra in the range $\lambda\lambda 1200$–$2000$. The ultraviolet spectra are shown in Figures 1 and 2, and exposure times and image numbers are in Table 1. For the Mg II spectra, corrections have been made for both the inter-order background flux and the blaze of the spectrograph. The short-wavelength spectra were reduced using the calibration of Cassatella *et al.* (1980). The emissions formed above a temperature of about 20,000 K, such as C II, C IV, Si IV, and N V are clearly visible in $\theta^1$ Tau and $\gamma$ Tau and not apparent in the long exposures of $\delta$ Tau and $\varepsilon$ Tau. (Fig. 1). The Mg II $h$ and $k$ emission is also stronger in $\theta^1$ Tau and $\gamma$ Tau compared with $\delta$ Tau and $\varepsilon$ Tau (Fig. 2).

Optical observations of Ca II K profiles were obtained with the 1.5 m reflector and echelle spectrograph at F. L. Whipple Observatory at Mt. Hopkins (Table 1). Digital spectra are recorded with an image-intensified, photon-counting Reticon array. The detector is a dual-lined $936 \times 2$ element array and permits a resolution of $\sim 0.04$ Å at Ca II K.

The spectra of the chromospheric Ca II K features and the surrounding photospheric region are shown in comparison to the *IUE* Mg II $h$ and $k$ spectra in Figure 2. In the data-reduction procedure for optical spectra (cf. Baliunas 1979; Baliunas and Dupree 1982) we have corrected for the fixed-pattern introduced in the detector system and the blaze function of the spectrograph by dividing the sum of several incandescent exposures obtained during the days bracketing the nighttime stellar observations. A thorium-argon emission spectrum is recorded before and after each stellar exposure, and a least squares fit to a seventh-order polynomial is computed to describe the wavelength calibration. In the

[1]Guest Investigator, *International Ultraviolet Explorer* satellite.

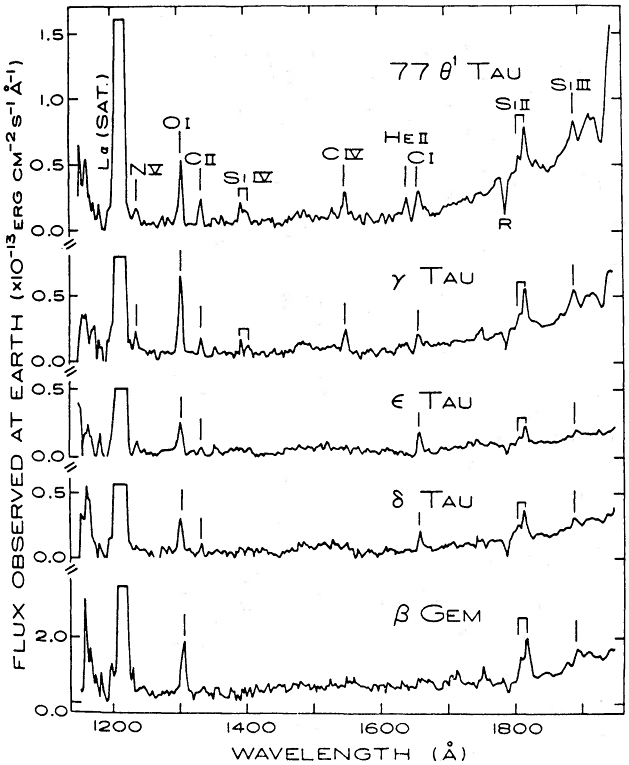


FIG. 1.— *IUE* short-wavelength, low-resolution spectra of the four Hyades giants and the field star $\beta$ Gem. The high-temperature, solar-like transition-region lines are clearly present in $\theta^1$ Tau and $\gamma$ Tau. The enhancement of the ultraviolet emissions is correlated with the strong Ca II and Mg II chromospheric emissions in these stars.

Ca II K spectra, no correction for scattered light or background illuminance has been made.

The behavior of the strength of the Ca II K emission is similar to that of Mg II *h* and *k*: the two Hyades giants $\theta^1$ Tau and $\gamma$ Tau both show stronger emission than $\delta$ Tau and $\epsilon$ Tau. The field giant $\beta$ Gem has a Ca II K emission strength comparable to those of $\epsilon$ Tau and $\delta$ Tau.

### III. ANALYSIS

For the comparison of the Hyades giants, we assume that the ultraviolet and optical chromospheric and transition-region emission emanates from the giant stars. Other possibilities will be discussed in a later section.

#### *a*) *Line Strengths*

From the ultraviolet spectra, the surface fluxes of the line emissions are calculated from angular diameters derived from the Barnes and Evans (1976) formulae and the broad-band magnitudes of the stars measured by Johnson *et al.* (1966). The observed fluxes and colors and the inferred surface fluxes are listed in Tables 2 and 3. The Mg II surface fluxes were measured from the high-resolution profiles by integration of the signal above zero and between the photospheric minimum flux at the base of the emission core. The calibration constant for the long-wavelength, high-dispersion spectra was determined by Baliunas (1979) and agrees with that of Hartmann, Dupree, and Raymond (1982) to within 5%. For that calibration, the flux obtained from Goddard extracted spectra is multiplied by 100. This factor forces agreement between sequential and, hence, nearly simultaneous high- and low-resolution Mg II fluxes measured in the G8 III–IV star $\lambda$ Andromedae.

The surface fluxes of the integrated emission in Mg II *h* and *k* have a range of about a factor of 2, as can be seen from Table 3. The Hyades giants $\theta^1$ Tau and $\gamma$ Tau are brightest in Mg II, while $\delta$ Tau and $\epsilon$ Tau, along with $\beta$ Gem, have lower integrated surface fluxes.

In the short-wavelength *IUE* spectra, the surface fluxes for $\theta^1$ Tau and $\gamma$ Tau are higher by factors of 2–5 than detections or upper limits of nondetections for the same lines in $\delta$ Tau, $\epsilon$ Tau, and $\beta$ Gem. Compared to the quiet Sun (see Table 2 and Fig. 3), the integrated surface fluxes in the strongest ultraviolet emission lines in $\theta^1$ Tau and $\gamma$ Tau are at most 2–3 times solar, while for $\delta$ Tau and $\epsilon$ Tau, the surface fluxes could be equal to the quiet-Sun values. For Mg II in the Hyades giants, the emission ranges from 30% to 50% of the quiet-Sun values.

The relative strength of the chromospheric Ca II K emission cores in these giants was studied with the following procedure. A second-order polynomial was least squares fitted to 2 Å of the Ca II K photospheric absorption profile on each side of the emission core. The emission in excess of this normalized continuum was numerically integrated to produce the emission strengths of Ca II K (labeled Ca II [K]) listed in Table 3. The photospheres of these stars are similar enough that the quadratic continuum ought to be a good analytic normalization procedure among the spectra. The strength of the emission will be related to the amount of radiative cooling present in the chromosphere. The measurement of Ca II [K] is not necessarily in proportion to the radiative cooling owing to the uncertainty of terms for the contributions of photospheric cooling and of scattered light in the spectra. The relative importance of the cooling, however, can still be discerned by comparing Ca II [K] among these giants. For $\theta^1$ Tau and $\gamma$ Tau, which show stronger chromospheric Ca II and Mg II emissions, the surface fluxes of the transition-region lines are correspondingly bright. The stars $\delta$ Tau, $\epsilon$ Tau, and $\beta$ Gem are weak in the high-temperature transition-region lines and in the chromospheric Ca II and Mg II emissions. Thus, the surface fluxes of the transition-region lines are enhanced as the chromospheric mechanical energy deposition increases, as evidenced by increased radiative losses in Mg II and Ca II.

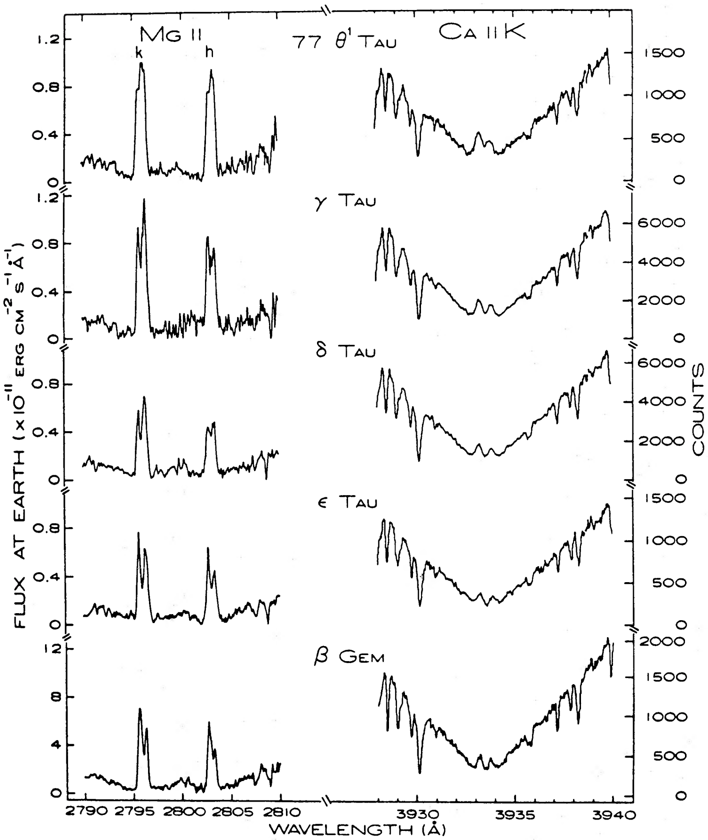


FIG. 2.—Mg II *h* and *k* (*left*) and Ca II K (*right*) profiles of the four Hyades giants $\theta^1$ Tau, $\gamma$ Tau, $\delta$ Tau, and $\varepsilon$ Tau and the field giant $\beta$ Gem. The chromospheric emission strengths are largest in $\theta^1$ Tau and $\gamma$ Tau.

This result has been previously found in late-type dwarfs (Hartmann *et al.* 1979). The same conclusion has also been drawn for a sample of dwarf, subgiant, and giant stars by Oranje, Zwaan, and Middelkoop (1982).

The Hyades giants $\delta$ Tau, $\gamma$ Tau, and $\theta^1$ Tau have been detected, with the *Einstein Observatory*, as X-ray sources (Stern *et al.* 1981; see Tables 1 and 3). The star $\varepsilon$ Tau is located outside the field of view of the X-ray survey and has not been observed. The X-ray surface flux of $\theta^1$ Tau is about a factor of 10 larger than in $\delta$ Tau; the C IV emission is correspondingly at least 6 times stronger in surface flux in $\theta^1$ Tau compared with the upper limit in $\delta$ Tau. Thus, the X-ray emission strength is correlated with the strengths of the high-temperature transition-region lines and the larger Mg II and Ca II chromospheric radiative losses. The weak-chromosphere stars $\varepsilon$ Tau and $\delta$ Tau presumably also have solar-like transition regions but at a level below our detection limit in the *IUE* spectra. Thus the ultraviolet and optical spectra may be used to predict the level of X-ray activity from these stars. It is striking that the ultraviolet and X-ray emissions have the same relative strength in these stars even though the observations were completed at different times. These giants must not have substantial changes in activity on a time scale shorter than about six months.

Another noteworthy feature of the spectrum of $\theta^1$ Tau is the appearance of He II ($\lambda$1640). This feature is associated with active-star spectra, such as dwarfs (Hartmann *et al.* 1979) or active giants, as in the case of $\lambda$ And, an RS CVn–type binary (Baliunas and Dupree 1982), which show coronal X-ray emission. The He II feature may be formed by EUV ionizations from X-rays over active regions (Hartmann *et al.* 1979).

### *b*) *Profile Asymmetries*

Asymmetries in the shapes of the emission cores of Ca II and Mg II may be interpreted as differential flows through the atmosphere in the line-forming regions. Outward flows, which are deduced from the line cores, may be interpreted as mass loss from the atmosphere (Stencel and Mullan 1980). In general, cool low-gravity stars that apparently possess cool winds show no signatures of gas at temperatures above $2 \times 10^4$ K (Linsky and Haisch 1979; Hartmann, Dupree, and Raymond

TABLE 1

SUMMARY OF OBSERVATION DATES OF THE HYADES GIANT STARS AND $\beta$ GEMINORUM

A. *IUE*—ULTRAVIOLET

| Star | Image Number | UT Date | Exposure Time (minutes) |
|---|---|---|---|
| $\theta^1$ (77) Tau ...... | SWP 4731 | 1979 Mar 23 | 110 |
| | SWP 6871 | 1979 Oct 15 | 80 |
| | LWR 5840 | 1979 Oct 15 | 20 |
| $\gamma$ Tau ........... | SWP 4701 | 1979 Mar 19 | 120 |
| | SWP 6880 | 1979 Oct 16 | 180 |
| | LWR 4070 | 1979 Mar 19 | 15 |
| | LWR 5865 | 1979 Oct 18 | 20 |
| $\delta$ Tau ........... | SWP 4702 | 1979 Mar 20 | 160 |
| | SWP 6879 | 1979 Oct 16 | 180 |
| | LWR 4071 | 1979 Mar 20 | 30 |
| | LWR 5845 | 1979 Oct 16 | 20 |
| $\varepsilon$ Tau ........... | SWP 4728 | 1979 Mar 22 | 120 |
| | SWP 6870 | 1979 Oct 14 | 180 |
| | LWR 4089 | 1979 Mar 22 | 30 |
| $\beta$ Gem .......... | SWP 4730 | 1979 Mar 23 | 20 |
| | LWR 4091 | 1979 Mar 23 | 3 |

B. WHIPPLE OBSERVATORY—VISIBLE

| Star | Sequence Number | UT Date |
|---|---|---|
| $\theta^1$ (77) Tau ... | 1112 | 1979 Oct 30 |
| $\gamma$ Tau ......... | 1113 | 1979 Oct 30 |
| $\delta$ Tau ......... | 1160 | 1979 Nov 4 |
| $\varepsilon$ Tau ......... | 1127 | 1979 Oct 31 |
| $\beta$ Gem ........ | 1222 | 1979 Dec 7 |

C. *HEAO 2*—X-RAY[a]

| Star | IPC Field Number | UT Date |
|---|---|---|
| $\theta^1$ (77) Tau ... | 3512 | 1979 Sep 17 |
| | 3513 | 1979 Sep 9 |
| $\gamma$ Tau ......... | 3663 | 1980 Feb 10 |
| | 3664 | 1980 Feb 10 |
| $\delta$ Tau ......... | 3519 | 1979 Mar 7 |
| $\varepsilon$ Tau ......... | n.a. | n.a. |
| $\beta$ Gem ........ | n.a. | n.a. |

[a]Stern *et al.* 1981 observations of three Hyades giants; "n.a." indicates no measurements are available.

1982). The shape of the Ca II and Mg II line profiles, if interpreted as the presence or absence of strong mass loss, is not consistent in explaining the discrepancy in the strength of the ultraviolet emissions in the Hyades giants. Asymmetries of the intensities of the emission peaks for Mg II and Ca II K are apparent from Figure 2 and are listed in Table 3. The asymmetry ascribed to each star for Mg II is determined by the Mg II $k$ feature, since the Mg II $h$ profile occurs at a low intensity point along the *IUE* spectrograph blaze function and is often underexposed and noisy. The influence of strong absorption caused by the interstellar medium gas has been ruled out as the reason for different asymmetries of Mg II among the Hyades giants. The stars all have heliocentric radial velocities of $+40$ km s$^{-1}$ (Abt and Biggs 1972). Because the Hyades is relatively nearby, a substantial radial velocity difference in the interstellar gas toward each of the giants in the cluster is unlikely, and any interstellar absorption feature should appear at the same wavelength in each star's profile. Since the profile asymmetries are different in $\varepsilon$ Tau compared with the other Hyades giants, the asymmetries for Mg II are inferred to be predominantly chromospheric in origin.

The Ca II K profiles all show that the intensity of the violet emission peak is slightly greater than that of the red peak, labeled $V > R$ in Table 3. The Mg II $k$ asymmetries are $v < r$, opposite that of Ca II K except

TABLE 2

*IUE* ULTRAVIOLET OBSERVATIONS OF HYADES GIANTS AND BETA GEMINORUM

| | | $\theta^1$ (77) Tau K0 IIIb[a] | | $\gamma$ Tau K0 IIIab | | $\delta$ Tau K0 III | | $\varepsilon$ Tau G9.5 III | | $\beta$ Gem K0 III | | Sun |
|---|---|---|---|---|---|---|---|---|---|---|---|---|
| FEATURE | λ(Å) | $f_\oplus$[b] | $f_\star/f_\odot$[c] | $f_\oplus$ | $f_\star/f_\odot$ | $f_\oplus$ | $f_\star/f_\odot$ | $f_\oplus$ | $f_\star/f_\odot$ | $f_\oplus$ | $f_\star/f_\odot$ | $f_\odot$[d] |
| N v ........ | 1240 | 0.7 | 2.7 | 0.7 | 2.4 | (0.2) | (0.8) | (0.4) | (1.4) | ... | ... | 0.85 |
| O I ......... | 1304 | 3.7 | 2.7 | 3.9 | 2.8 | 2.1 | 1.6 | 2.1 | 1.5 | 13.3 | 0.9 | 4.0 |
| C II ........ | 1335 | 1.0 | 0.7 | 0.5 | 0.3 | (0.3) | (0.2) | (0.3) | (0.4) | ... | ... | 4.6 |
| Si IV ....... | 1394, 1403 | 1.6 | 2.0 | 0.9 | 0.5 | (0.3) | (0.2) | (0.5) | (0.4) | ... | ... | 2.0 |
| C IV ........ | 1550 | 1.6 | 0.9 | 1.5 | 0.7 | (0.3) | (0.1) | (0.3) | (0.2) | (2.2) | (0.1) | 5.8 |
| He II ....... | 1640 | 1.0 | 2.5 | (0.5) | (1.2) | ... | ... | ... | ... | ... | ... | 1.3 |
| C I ......... | 1657 | 1.3 | 0.8 | 1.0 | 0.5 | 0.9 | 0.6 | 1.7 | 0.9 | (1.2) | (0.1) | 5.3 |
| Si II ........ | 1808, 1817 | 6.9 | 1.4 | 2.5 | 0.4 | 2.3 | 0.4 | 0.8 | 0.2 | 4.0 | 0.1 | 16.1 |
| Si III ....... | 1892 | 0.8 | ... | 0.8 | ... | 0.5 | ... | (0.3) | ... | (2.3) | ... | ... |
| Mg II *k* .... | 2796 | 104.0 | ... | 115.0 | ... | 61.9 | ... | 67.3 | ... | 586. | ... | ... |
| | | | 0.5 | | 0.5 | | 0.3 | | 0.3 | | 0.2 | 1240. |
| Mg II *h* .... | 2802 | 86.5 | ... | 85.0 | ... | 49.3 | ... | 52.0 | ... | 450. | ... | ... |
| $V^e$ ......... | | 3.83 | | 3.65 | | 3.76 | | 3.54 | | 1.14 | | |
| $(V-R)^e$... | | 0.71 | | 0.73 | | 0.73 | | 0.73 | | 0.75 | | |

[a]Spectral classification from Keenan and Pitts 1980.

[b]Flux observed at Earth in units of $10^{-13}$ ergs cm$^{-2}$ s$^{-1}$. Listed fluxes are sometimes the average from two exposures. Upper limits are given in parentheses.

[c]Ratio of stellar surface flux (see Table 2) to quiet-Sun surface flux. Upper limits are given in parentheses. The sum of the Mg II $(h+k)$ emission is listed.

[d]Quiet-Sun surface fluxes are from G. Rottman (quoted by Linsky *et al.* 1978), in units of $10^3$ ergs cm$^{-2}$ s$^{-1}$.

[e]$V$-magnitude and $(V-R)$ color used to calculate the surface fluxes are from Johnson *et al.* 1966.

for $\varepsilon$ Tau, which shows $v > r$ in Mg II and Ca II. Variation in the line profiles may be an explanation for the apparent inconsistency in the Ca II and Mg II asymmetries in three of the giants, because the optical and ultraviolet spectra are not simultaneous. We have monitored the Ca II profiles in these stars during six months in 1979, and we detected no changes in the relative shapes of the line profiles and no variations in the relative flux in the core to within 5%. No significant changes (greater than 5% in the flux) are present, either, in two Mg II exposures of each of the Hyades giants obtained in 1979. The asymmetries for Ca II and Mg II, however, can be discrepant in cool giants, as noted by Stencel and Mullan (1980).

The spread in chromospheric and coronal emissions among the Hyades giants is based on something other than location in the H-R diagram, contrary to the sharp "dividing line" proposed by Linsky and Haisch (1979). A blurring of the transition of mass loss indicators is also suggested by observations of the hybrid-atmosphere supergiants $\alpha$ Aqr and $\beta$ Aqr (Hartmann, Dupree, and Raymond 1980) and, further, by the smooth transition of fluxes of ultraviolet features in giants in a range of spectral types (Oranje, Zwaan, and Middelkoop 1982). It is the *abruptness* of the transition of mass loss indicators which is offered as a consistency argument by Stencel and Mullan (1980) in favor of a sharp dividing line of ultraviolet emission in the H-R diagram. The Hyades giants underscore the blurring of these dividing lines in a unique way by suggesting other parameters besides location in the H-R diagram in controlling chromospheric and coronal emission. These stars provide the strongest evidence in the search for fundamental determinants of activity.

## IV. DISCUSSION

The most striking result of the data presented here is the dissimilarity in chromospheric and coronal emissions for stars ostensibly similar in photospheric properties. We discuss possible causes for the discrepancies in the ultraviolet emissions.

### *a*) *Binary Companions*

Both $\delta$ Tau and $\theta^1$ Tau have been reported as single-lined spectroscopic binaries with very long periods (Griffin and Gunn 1977). These periods are on the order of 530 days for $\delta$ Tau and probably near 6000 days for $\theta^1$ Tau. Although $\gamma$ Tau has been resolved into two components by speckle interferometry, no information is available on the nature of the companion star (Morgan *et al.* 1982). The companions are most likely dwarf stars with substantial orbit separations; the primary stars show sharp photospheric lines indicative of slow projected rotational velocities, as discussed below. Thus the Hyades giants are not related to the RS CVn–type close binary systems with relatively rapid rotational velocities

TABLE 3

SUMMARY OF CHROMOSPHERIC AND CORONAL EMISSIONS OF HYADES GIANTS AND BETA GEMINORUM

A. *IUE*—ULTRAVIOLET

| Feature | λ (Å) | $\theta^1$ Tau $f_\star$[a] | γ Tau $f_\star$ | δ Tau $f_\star$ | ε Tau $f_\star$ | β Gem $f_\star$ |
|---|---|---|---|---|---|---|
| N V | 1240 | 2.3 | 2.0 | (0.7) | (1.2) | ... |
| O I | 1304 | 12.0 | 11.0 | 6.4 | 5.9 | 3.7 |
| C II | 1335 | 3.2 | 1.5 | (0.8) | (0.8) | ... |
| Si IV | 1394, 1403 | 5.2 | 2.4 | (0.8) | (1.5) | ... |
| C IV | 1550 | 5.2 | 4.1 | (0.8) | (0.8) | (0.6) |
| He II | 1640 | 3.2 | (1.5) | ... | ... | ... |
| C I | 1657 | 4.2 | 2.7 | 2.9 | 4.6 | (0.3) |
| Si II | 1808, 1817 | 22.4 | 7.0 | 7.0 | 2.2 | 1.1 |
| Si III | 1892 | 2.6 | 2.3 | 1.6 | (0.8) | (0.6) |
| Mg II ($h+k$) | 2802, 2796 | 587. | 566. | 345. | 334. | 290. |
| Mg II asymmetries[b] | | $v < r$ | $v < r$ | $v < r$ | $v > r$ | $v > r$ |

B. VISIBLE

| Feature | λ (Å) | [K][c] | [K] | [K] | [K] | [K] |
|---|---|---|---|---|---|---|
| Ca II K | 3934 | 0.60 | 0.48 | 0.26 | 0.18 | 0.24 |
| Ca II K asymmetries[b] | | $V > R$ | $V > R$ | $V > R$ | $V > R$ | $V > R$ |

C. *HEAO 2*—X-RAY

| Feature | λ (Å) | $\theta^1$ Tau | γ Tau | δ Tau | ε Tau | β Gem |
|---|---|---|---|---|---|---|
| log $L_x$[d] | | 30.0 | 29.4 | 28.9 | n.a. | n.a. |

[a]Surface fluxes in units of $10^3$ ergs cm$^{-2}$ s$^{-1}$. The fluxes have been calculated by attributing the emission to the giant stars in the cases of binary systems.

[b]Relative intensities of the violet and red emission peaks of the Mg II $k$ emission profile (with peaks labeled $v$ and $r$) and Ca II K (peaks labeled $V$ and $R$).

[c]Ratio of integrated emission, in units of Å, in the line core to the base of the emission core, where the base of the emission core is defined as unity.

[d]*HEAO 2* observations of three Hyades giants from Stern *et al.* 1981. The logarithmic stellar surface luminosities are given; "n.a." indicates no measurements are available.

and strong chromospheric and coronal emission as compared with their more slowly rotating, single-star counterparts.

There is no direct evidence from which to conclude whether the ultraviolet and X-ray emissions emanate from the giants or from the unseen, binary companions of the giants. Indirect evidence, however, suggests that the giants are responsible for the ultraviolet and X-ray emissions.

We first estimate the spectral types of the companions reported for $\theta^1$ Tau, γ Tau, and δ Tau from the presence of continuum flux in the short-wavelength *IUE* spectra in Figure 1. For the Hyades giants, ε Tau shows the flattest continuum in the region of λ1800. We can assume that the *IUE* continuum spectrum of ε Tau near λ1800 represents that of a K0 III star. In comparison, $\theta^1$ Tau, γ Tau, and δ Tau show slightly steeper continuum slopes toward the longer wavelengths around λ1800. We can estimate the spectral types of the secondary companions by comparing the excess flux in those three giants with that of ε Tau and by assuming that all four Hyades giants have the same intrinsic ultraviolet colors. The excess flux includes a contribution from scattered photospheric light. The excess flux thus gives an upper limit to the stellar flux, which, in turn, implies the earliest spectral type of the secondary star. The ratio of excess flux for $\theta^1$ Tau, γ Tau, and δ Tau to that for ε Tau is corrected for the slight differences in $V$-magnitude among the stars. The types of the presumed companions are deduced from the ultraviolet colors of Wu *et al.* (1980). For $\theta^1$ Tau, lunar occultation measures provide us with the $V$-magnitude difference between the primary and secondary, $\Delta V = 3.5$ (Peterson *et al.* 1981). The magnitude difference and ultraviolet continuum excess imply a spectral type of F6 V or later for the secondary in $\theta^1$ Tau. Peterson *et al.* also measure the visible colors of the secondary during the lunar occultation and derive a spectral type of the secondary in the range G0–G5 V. For the companions of δ Tau and γ Tau, there are no measurements for $\Delta V$. If we assume a range $\Delta V = 3.0$–$4.0$, which is typical for the Hyades main sequence, then the apparent excess continuum flux at λ1800 implies a secondary star for δ Tau in the range F8–G0 V, while for the companion to γ Tau, F6–F8 V.

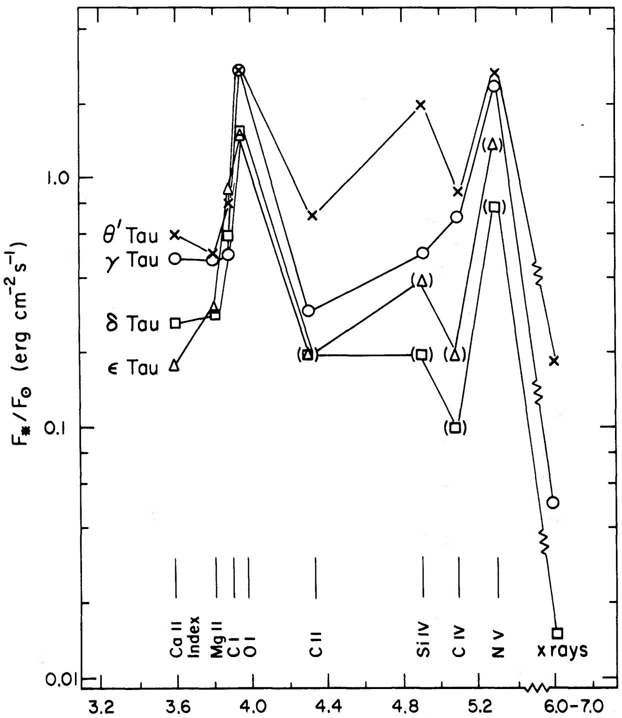


FIG. 3.—The surface flux in individual chromospheric and transition-region lines and soft X-rays, relative to that of the quiet Sun as a function of temperature of formation. The X-ray fluxes for the Hyades are from Stern *et al.* (1981); a solar X-ray flux of $5.5 \times 10^5$ ergs cm$^{-2}$ s$^{-1}$ was adapted from the mean of quiet and active values (Vaiana and Rosner 1978).

Is the chromospheric and coronal emission consistent with the spectral type of the companion in $\theta^1$ Tau? The X-ray luminosity observed with *Einstein* (Stern *et al.* 1981) is comparable to that observed for the G0 V Hyades star BD+14°693. The surface flux measured from a mid-F dwarf secondary instead of K0 III primary would be about 30 times that of the quiet Sun in C IV—the observed C IV flux is 20 times the solar value for BD+14°693, in rough agreement (Baliunas 1981, private communication). Although this flux level might be expected from an active, young Hyades dwarf, we prefer to attribute the activity to the giant stars for several reasons. First, the Mg II and Ca II emissions arise from the giants, deduced from the width of the emission cores and the Wilson-Bappu effect. It is reasonable to assume, since the Mg II and Ca II emissions of the *giants* $\theta^1$ Tau and $\gamma$ Tau are enhanced relative to $\delta$ Tau and $\varepsilon$ Tau, that the giants are also responsible for the enhanced ultraviolet and X-ray emissions. Second, we note that most of the Hyades dwarfs have $L_x \sim 10^{29}$ ergs s$^{-1}$; $L_x \sim 10^{30}$ ergs s$^{-1}$ is observed in only two out of $\sim 40$ dwarfs detected or with upper limits. Thus it would require an unusually X-ray–bright dwarf to explain the X-ray luminosity of $\theta^1$ Tau; $\gamma$ Tau is similarly on the high-luminosity end of the X-ray luminosity distribution.

Finally, we note that active dwarfs show enhancements from solar surface flux levels which are higher in C IV than in O I (cf. Hartmann, Dupree, and Raymond 1982). For example, observations of BD+14°693 show a C IV surface flux $\sim 16$ times the solar value, while O I is only 10 times solar (Baliunas 1981, private communication). In contrast to these observations of active dwarf stars, the Hyades giants with measured C IV all exhibit O I enhancements much greater than C IV, so that any hypothesized dwarf star would have to have an enhancement of the O I/C IV ratio of about 1.5. This behavior of the O I to C IV ratio is more consistent with *IUE* observations of low-gravity stars, which show increases in O I fluxes from the increased fluorescence with Ly$\beta$ in extended chromospheres as compared with the higher gravity stars (Hartmann, Dupree, and Raymond 1982). We conclude that the ultraviolet and X-ray emissions arise from the giant components themselves.

### *b*) *Rotation*

The photospheric lines in the region surrounding Ca II K are fairly sharp, which indicates small projected rotational velocities for these giants. Among dwarfs, rotation is a trademark of enhanced chromospheric emission (Kraft 1967). The Hyades dwarfs are relatively younger and more rapidly rotating than comparable field dwarfs; their chromospheric emissions are also correspondingly stronger. For evolved stars in the field, Oranje, Zwaan, and Middelkoop (1982) find a similar relation between increasing strength of the surface fluxes of chromospheric and transition-region emissions and increasing projected rotational velocity. The dispersion of this relation, however, is large and is typified by the Hyades giants.

The projected rotational velocities, $v \sin i$, for the Hyades giants are less than 6 km s$^{-1}$ according to Kraft (1967); the velocities lie beneath the level of detection of Kraft's high-dispersion spectrum line-broadening measurements. We have investigated any differences in the projected rotational velocities among the Hyades giants with the following technique.

With $\beta$ Gem as a spectrum template in our echelle spectra, we calculated the cross-correlation coefficient as a function of wavelength in the spectra of each of the Hyades giants. This technique has been successfully employed in the determination of galaxy velocity dispersions (cf. Tonry and Davis 1979). The width of the primary peak of the cross-correlation shows excess broadening in the photospheric lines of the Hyades giants.

The projected rotational velocity of $\beta$ Gem, 2.2 km s$^{-1}$, is presumed correct as measured by Gray and Martin (1979). Excess broadening of the cross-correlation peaks of $\beta$ Gem above that of the Hyades giants is

TABLE 4

MEASUREMENTS OF PROJECTED ROTATIONAL VELOCITIES IN THE HYADES GIANTS AND BETA GEMINORUM

| | $v \sin i$ (km $s^{-1}$) | |
|---|---|---|
| STAR | This Work | Gray and Endal 1982 |
| $\theta^1$ (77) Tau ......... | 2.7 | 2.4 |
| $\gamma$ Tau................ | 2.9 | 3.4 |
| $\delta$ Tau................ | 2.7 | 1.9 |
| $\epsilon$ Tau................ | 3.0 | 3.4 |
| $\beta$ Gem ............. | [2.2][a] | ... |

[a] This rotational velocity, from Gray and Martin 1979, is presumed in our differential technique.

attributed to rotational broadening. In order to convert the excess broadening in the cross-correlation peaks to rotational broadening, we calibrate the excess broadening of correlations from spectra for stars whose projected rotational velocities are assumed known. The late-type stars from which we calibrate projected rotational velocities are $\alpha$ Tau (K0 III, $v \sin i = 2.7$ km $s^{-1}$; Smith and Dominy 1979), $\alpha$ Boo (K2 III, $v \sin i = 2.7$ km $s^{-1}$; Smith and Dominy 1979), and $\alpha$ CMi (F5 IV, $v \sin i = 3.5$ km $s^{-1}$; Wynne-Jones, Ring, and Wayte 1978). We also rely on the knowledge that the contribution to excess broadening due to photospheric differences between $\beta$ Gem and the Hyades giants is small, and macro- and micro-turbulent velocities for a range of late-type stars are similar (Smith 1979; Soderblom 1982). The results for the Hyades giants (see Table 4) show that the widths of the cross-correlation peaks are extremely similar—within 1 km $s^{-1}$ of each other. The low projected rotational velocities of the giants makes it difficult to assign an accurate $v \sin i$. This comparative analysis has subsumed the subtle differences between the competing influences of the effects of, for example, macroturbulence and microturbulence; thus the width of the cross-correlation peak can only be roughly dissected for $v \sin i$. Our velocities, however, are similar to the rotational velocities for the Hyades giants determined by Gray and Endal (1982) and included in Table 4. In their technique, high-resolution, high signal-to-noise photospheric line profiles are decomposed by Fourier analysis into components of microturbulence, macroturbulence, and rotation. They estimate errors of $\pm 0.5$ km $s^{-1}$ for their values of $v \sin i$. The projected rotational velocities from the two methods agree to within the quoted uncertainty of 0.5 km $s^{-1}$ for three of the Hyades giants; the exception is $\delta$ Tau. According to Gray and Endal, $\delta$ Tau has the narrowest photospheric lines of the giants, which yields a $v \sin i$ near our resolution limit. Our result for $\delta$ Tau may thus be an upper limit to the rotational velocity.

The result of these analyses of rotational velocity suggest that the Hyades giants likely have values of $v \sin i$ which are small and similar one to another. If rotation were to be invoked as the explanation for the range of chromospheric and coronal emissions in the Hyades, then either a discontinuity in the decrease of emission strength with slower rotational velocity or a fortuitous projection of the rotation axes is required, such that more rapid rotation is masked in $\theta^1$ Tau and $\gamma$ Tau.

### c) *Photospheric Differences*

The spectral types, or temperatures and gravities, of these giants have been determined by several investigators (cf. Boesgaard, Heacox, and Conti 1977; Gray and Endal 1982). If we assume that the MK spectral types are precise and order the giants in decreasing photospheric temperature, then the two hottest Hyades giants, $\theta^1$ Tau and $\gamma$ Tau, are also the brightest in chromospheric and coronal emissions. However, other investigators invert the order of the photospheric temperatures, and the error in assigning a spectral type appears to be about one subclass, which incorporates the spread of all the Hyades giants from K0. Photospheric temperature differences, if real, appear to be 200 K *at most*. The possibility of a hidden agent which exerts a strong control on chromospheric and coronal emissions in the giants remains. However, such an agent, if controlled by the subtle photospheric differences in these giants, would have a peculiarly sharp dependence near spectral type K0 III.

### d) *Possibility of Long-Term Variations*

A range of chromospheric and coronal emissions is observed for the Hyades giants, a sample of four coeval stars with apparently similar photospheric properties. The range of emissions from these stars is not easily explained by differences in macroscopic parameters such as age, rotation rate, or photospheric properties among these stars.

From this study of the Hyades giants, a possible explanation for the chromospheric differences in the Hyades giants is a spread due to activity cycles—$\theta^1$ Tau and $\gamma$ Tau may be very active now, $\delta$ Tau and $\epsilon$ Tau less so. There is some circumstantial evidence that giants near spectral type K0 may undergo time variations, possibly cyclic, in chromospheric Ca II H and K emission. Wilson (1982) and Middelkoop (1982) have surveyed field giants for chromospheric emission and also find a wide scatter of the chromospheric emission near the color of the Hyades giants. Since these measurements comprise a snapshot survey, the scatter in the measurements of Ca II H and K could be interpreted as variability arising from the sampling of random phases. There is intrinsic uncertainty in their sample because field stars are a heterogeneous group; it is difficult to identify activity cycles as the sole reason for the observed spread in emission.

Our observations of the Hyades, a homogeneous stellar sample, substantially reduces the number of free parameters and appears to give the first evidence for long-term activity cycles among giant stars. That such cycles exist among dwarf stars is well documented (Wilson 1978). These results for the Hyades establish a baseline from which to embark on long-term monitoring of luminous stars.

This research is supported in part by the Langley-Abbot program of the Smithsonian Institution and by NASA grants NSG 5370 and NAG 5-87.

REFERENCES

Abt, H., and Biggs, E. S. 1972, *Bibliography of Stellar Radial Velocities* (Tucson: Kitt Peak National Observatory).
Baliunas, S. L. 1979, Ph.D. thesis, Harvard University.
Baliunas, S. L., and Dupree, A. K. 1982, *Ap. J.*, **252**, 668.
Barnes, T. G., and Evans, D. S. 1976, *M.N.R.A.S.*, **174**, 489.
Boesgaard, A. M., Heacox, W. D., and Conti, P. S. 1977, *Ap. J.*, **214**, 124.
Cassatella, A., Holm, A., Ponz, D., Schiffer, F. H., III. 1980, *IUE-ESA Newsletter*, No. 5.
Gray, D. F., and Endal, A. S. 1982, *Ap. J.*, **254**, 162.
Gray, D. F., and Martin, B. 1979, *Ap. J.*, **231**, 139.
Griffin, R. E., and Gunn, J. E. 1977, *A.J.*, **82**, 176.
Hartmann, L., Davis, R., Dupree, A. K., Raymond, J., Schmidtke, P. C., and Wing, R. F. 1979, *Ap. J. (Letters)*, **233**, L69.
Hartmann, L., Dupree, A. K., and Raymond, J. C. 1980, *Ap. J. (Letters)*, **236**, L143.
______. 1982, *Ap. J.*, **252**, 214.
Johnson, H. L., Mitchell, R. I., Iriante, B., and Wisniewski, W. Z. 1966, *Comm. Lunar and Planet. Lab.*, **4**, 99.
Keenan, P. C., and Pitts, R. E. 1980, *Ap. J. Suppl.*, **42**, 541.
Kraft, R. P. 1967, *Ap. J.*, **150**, 551.
Lambert, D. L., Dominy, J. F., and Sivertsen, S. 1980, *Ap. J.*, **235**, 114.
Linsky, J. L., *et al.* 1978, *Nature*, **275**, 389.
Linsky, J. L., and Haisch, B. M. 1979, *Ap. J. (Letters)*, **229**, L27.
Middelkoop, F. 1982, *Astr. Ap.*, **113**, 1.
Morgan, B. L., Bechmann, G. K., Scadden, R. J., and Vine, H. A. 1982, *M.N.R.A.S.*, **198**, 817.
Oranje, B. J., Zwaan, C., and Middelkoop, F. 1982, *Astr. Ap.*, **110**, 30.
Peterson, D. M., Baron, R. L., Dunham, E., Mink, D., Weekes, T. C., and Elliot, J. L. 1981, *A.J.*, **86**, 280.
Smith, M. A. 1979, *Pub. A.S.P.*, **91**, 737.
Smith, M. A., and Dominy, J. F. 1979, *Ap. J.*, **231**, 477.
Soderblom, D. 1982, *Ap. J.*, **263**, 239.
Stencel, R. E., and Mullan, D. J. 1980, *Ap. J.*, **238**, 221.
Stern, R. A., Zolcinski, M.-C., Antiochos, S. K., and Underwood, J. H. 1981, *Ap. J.*, **249**, 647.
Tonry, J., and Davis, M. 1979, *A.J.*, **84**, 1511.
Vaiana, G. S., and Rosner, R. 1978, *Ann. Rev. Astr. Ap.*, **16**, 393.
Wilson, O. C. 1978, *Ap. J.*, **226**, 379.
______. 1982, *Ap. J.*, **257**, 179.
Wu, C.-C., Faber, S. M., Gallagher, J. S., Peck, M., and Tinsley, B. 1980, *Ap. J.*, **237**, 290.
Wynne-Jones, I., Ring, J., and Wayte, R. C. 1978, *Proceedings of the Fourth International Colloquium on Astrophysics*, ed. M. Hack (Trieste: Osservatorio Astronomico di Trieste), p. 519.

S. L. BALIUNAS, A. K. DUPREE, and L. HARTMANN: Harvard-Smithsonian Center for Astrophysics, 60 Garden Street, Cambridge, MA 02138